

Eksp. Teor. Fiz. 65, 1045 (1973) [Sov. Phys. JETP 38, 517 (1974)].

<sup>7</sup>N. I. Bul'ko, V. I. Kariman, and O. A. Pokhotelov, Preprint IZMIRAN No. 9, 1971; Pis'ma Zh. Eksp. Teor. Fiz. 14, 469 (1971) [JETP Lett. 14, 320 (1971)].

<sup>8</sup>N. N. Bogolyubov and Yu. A. Mitropol'skii, Asimptoticheskie metody v teorii nelineĭnykh kolebaniĭ (Asymptotic Methods in the Theory of Nonlinear Oscillations), Fizmatgiz, 1963.

<sup>9</sup>I. S. Gradshteĭn and I. M. Ryzhik, Tablitsy integralov, summ, ryadov i proizvedenĭ (Tables of Integrals, Sums, Series and Products), Fizmatgiz, 1963 [Academic, 1966].

<sup>10</sup>L. D. Landau and E. M. Lifshitz, Elektrodinamika sploshnykh sred (Electrodynamics of Continuous Media), Gostekhizdat, 1957 [Pergamon, 1959].

Translated by J. G. Adashko

## Raman scattering spectra and structural phase transitions in the improper ferroelastics $\text{Hg}_2\text{Cl}_2$ and $\text{Hg}_2\text{Br}_2$

C. Barta,<sup>1)</sup> A. A. Kaplyanskiĭ, V. V. Kulakov, B. Z. Malkin,<sup>2)</sup> and Yu. F. Markov

A. F. Ioffe Physico-technical Institute, USSR Academy of Sciences  
(Submitted October 20, 1975)  
Zh. Eksp. Teor. Fiz. 70, 1429-1444 (April 1976)

The Raman scattering (RS) spectra of crystals of the homologous calomel series, possessing at room temperature a tetragonal structure with a single linear molecule  $\text{Hg}_2\text{X}_2$  ( $\text{X} = \text{Cl}, \text{Br}, \text{I}$ ) in the primitive cell (space group  $D_{4h}^{17}$ ) are investigated in the 10 to 300°K temperature range. When the crystals are cooled below  $T_c = 185^\circ\text{K}$  ( $\text{Hg}_2\text{Cl}_2$ ) or  $T_c = 143^\circ\text{K}$  ( $\text{Hg}_2\text{Br}_2$ ) the RS spectra undergo a number of qualitative changes (appearance of new lines and splitting of degenerate oscillations), which point to a structural transition of the lattice to the orthorhombic phase  $D_{2h}^{17}$  with a double unit cell. Polarization of the RS spectral lines of the low-temperature phase is measured in samples made monodomain by uniaxial compression. The structural transition is analyzed within the framework of the phenomenological Landau theory of second-order phase transitions. It is shown that in  $\text{Hg}_2\text{X}_2$  crystals a transition of the displacement type is due to lattice instability with respect to oscillations from the acoustic transverse branch (soft mode) at two non-equivalent  $X$ -points on the boundary of the Brillouin zone of the tetragonal phase. The transition is characterized by a two-component order parameter and is accompanied by a spontaneous strain in the basal plane of the  $D_{4h}^{17}$  lattice ("improper" ferroelastic). Five of the six new RS-spectrum lines predicted by the theory are found below  $T_c$ . The intensities of the new lines (normalized by taking into account the temperature dependence of the phonon occupation numbers) and widths of the doublet splitting are linear functions of the squared frequency of the soft mode. The parameters of the model thermodynamic potential for calomel are determined from data on the dependence of the soft-mode frequency on the temperature, on the uniaxial compression, on the magnitude of spontaneous strain, and on the monodomainization threshold stress. The jumps in the specific heat and elastic constants at the transition point are estimated.

PACS numbers: 78.30.Gt, 64.70.Kb

A new interesting group of materials, halides of monovalent mercury,  $\text{Hg}_2\text{X}_2$ ,  $\text{X} = \text{Cl}, \text{Br}, \text{I}$ , was recently synthesized<sup>[1]</sup> in the form of synthetic single crystals. These isomorphous compounds have a unique crystal structure at 20 °C, consisting of parallel chains of linear molecules  $\text{Hg}_2\text{X}_2$ , which are relatively weakly coupled to one another. The molecules form a body-centered tetragonal lattice  $D_{4h}^{17}$  with one molecule per unit cell.<sup>[2]</sup> The chain structure of the  $\text{Hg}_2\text{X}_2$  crystals leads to an extraordinarily strong anisotropy of their physical properties. Thus, the crystals of calomel ( $\text{Hg}_2\text{Cl}_2$ ) have a very large elastic anisotropy (one of the sound velocities is the lowest of the velocities known in the condensed phase and is comparable with  $v_s$  in air<sup>[3]</sup>), and has a record value of optical birefringence ( $\Delta n = +0.65$ <sup>[4]</sup>). In<sup>[5,6]</sup>, investigations were made also of the spectroscopic properties of  $\text{Hg}_2\text{X}_2$  single crystals, namely the IR spectra and the Raman scattering (RS) spectra.

The study of the RS spectra has revealed<sup>[7]</sup> that at temperatures lower than  $T_c = 185 \text{ K}$  ( $\text{Hg}_2\text{Cl}_2$ ) and  $T_c = 143 \text{ K}$  ( $\text{Hg}_2\text{Br}_2$ ) they undergo a number of qualitative changes that point to a phase transition. The main effect consists in the appearance, in the first-order RS spectra, of additional weak lines at  $T \leq T_c$ , which are missing at  $T > T_c$ .<sup>[7]</sup> The existence of a phase transition was directly confirmed by observation of the domain structure of  $\text{Hg}_2\text{Cl}_2$  and  $\text{Hg}_2\text{Br}_2$  at  $T < T_c$ .<sup>[8]</sup> According to<sup>[8]</sup>, at  $T \leq T_c$  the tetragonal point group of the crystal  $D_{4h}$  is lowered to the centrosymmetrical orthorhombic group  $D_{2h}$ , with onset of spontaneous deformation; the samples can become single-domain by uniaxial compression (a "pure" ferroelastic).

In this paper, to explain the microscopic nature of the phase transition in  $\text{Hg}_2\text{X}_2$ , we report a detailed investigation of the RS spectra of the compounds  $\text{Hg}_2\text{Cl}_2$  and  $\text{Hg}_2\text{Br}_2$  at  $T \leq T_c$ . The clear-cut manifestation of

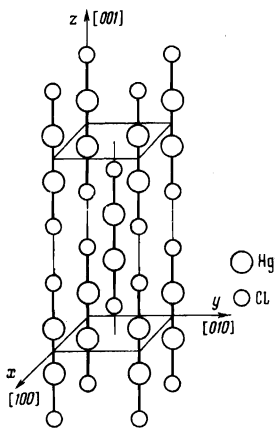


FIG. 1. Unit cell of  $\text{Hg}_2\text{Cl}_2$ .

the phase-transition effect in these spectra, particularly the observation of the soft mode,<sup>[9]</sup> has made it possible to interpret in detail the nature of the transition in  $\text{Hg}_2\text{X}_2$ . It is shown that it is the structure transition  $D_{4h}^{17} - D_{2h}^{17}$  with doubling of the unit cell. The transition is due to phonon instability, at  $T \leq T_c$ , of the transverse acoustic branch of the vibrational spectrum at the point X on the boundary of the tetragonal-phase Brillouin zone (improper ferroelectric). The Landau thermodynamic theory has been developed for a second-order transition in  $\text{Hg}_2\text{X}_2$  as in an improper ferroelastic with a two-component transition parameter. The parameters of the thermodynamic potential were determined from comparison with experiment and used to calculate the discontinuities of a number of physical quantities in the transition.

### 1. EXPERIMENTAL INVESTIGATION OF RS SPECTRA

A group-theoretical analysis<sup>[5,6]</sup> of the fundamental vibrations of the  $D_{4h}^{17}$  tetragonal lattice sets out from a

crystal structure in which the linear molecules  $\text{Hg}_2\text{X}_2$  form a body-centered tetragonal (BCT) lattice with one molecule per unit cell (Fig. 1). The table lists the results of this analysis: the symmetry of the oscillations at the point  $\Gamma$  (column 3) and the selection rules (column 2). The theory predicts four frequencies of the even oscillations active in the RS spectra, and two frequencies of the odd oscillations active in the IR spectra. The experimental results on the IR spectra<sup>[5]</sup> and on the first-order RS spectra<sup>[6]</sup> at 20 °C are in full agreement with the conclusions of the theory. The experimental values of the fundamental frequencies are given in column 1 of the table.<sup>3)</sup> The frequencies observed in the RS spectra pertain to the libration ( $\nu_1$ ), deformation ( $\nu_2$ ), and valent ( $\nu_3, \nu_4$ ) vibrations of the molecules.

The temperature dependences of the first-order RS spectra of the crystals  $\text{Hg}_2\text{Cl}_2$  and  $\text{Hg}_2\text{Br}_2$  were investigated in the interval from 300 °K to helium temperatures ( $T \approx 10^\circ\text{K}$ ), including the critical points  $T_c$ . The RS spectra were recorded with a "Coderg-PHO" double monochromator using a "Spectra Physics" 60-mW He-Ne laser. To determine the scattering tensor, the measurements were made at a 90° geometry of observation in polarized light on oriented single crystals. The crystal drawing procedure was described in<sup>[11]</sup>. They were oriented on the basis of the perfect cleavage of tetragonal crystals on the (110) and (1 $\bar{1}$ 0) planes. At  $T > T_c$ , the tensor was determined in terms of tetragonal axes  $x$ ,  $y$ , and  $z$  parallel to [100], [010], [001] respectively (Fig. 1).

The polarization of the RS spectra of  $\text{Hg}_2\text{X}_2$  crystals in the low-temperature orthorhombic phase was investigated at  $T = 77^\circ\text{K} \ll T_c$  on single-domain samples. The single-domain state was induced by uniaxial compression of the single crystals at 77 °K along [110] (Fig. 1), with the single-domain state preserved after

Fundamental frequencies and vibration symmetries of  $\text{Hg}_2\text{X}_2$  crystals.

Phase $D_{4h}^{17} (T > T_c)$		Phase $D_{2h}^{17} (T < T_c)$							
$T = 300\text{ K}$		$\alpha_{ik}, M_i$	$\Gamma (D_{4h})$	$X_1 (D_{2h})$	$\Gamma \rightarrow \Gamma$	$X_1 \rightarrow \Gamma$	$\alpha_{ik}, M_i$	$T = 90\text{ K}$	
$\text{Hg}_2\text{Cl}_2$	$\text{Hg}_2\text{Br}_2$							$\text{Hg}_2\text{Cl}_2$	$\text{Hg}_2\text{Br}_2$
1	2*	3	4	5	6	7*	8		
RS frequencies, $\text{cm}^{-1}$ [6]									
$\nu_1 = 40$	35, 6	$zx, zy$	$E_g$	$B_{2g} + B_{3g}$	$B_{2g} + B_{3g}$	$A_u + B_{1u}$	Z	—	—
$\nu_2 = 137$	91	$zx, zy$	$E_g$	$B_{2g} + B_{3g}$	$B_{2g} + B_{3g}$	$A_u + B_{1u}$	Z	—	—
$\nu_3 = 167$	135	$zz, xx + yy$	$A_{1g}$	$A_g$	$A_g$	$B_{3u}$	X	—	—
$\nu_4 = 275$	221	$zz, xx + yy$	$A_{1g}$	$A_g$	$A_g$	$B_{3u}$	X	—	—
IR frequencies, $\text{cm}^{-1}$ [6]									
$\nu_5^T = 67$	47	$x, y$	$E_u TO$	$B_{3u}$	$B_{3u}$	$A_g$	$XX, YY, ZZ$	$\nu_5^T = 72$	52
$\nu_5^L = 135$	94	—	$E_u LO$	$B_{2u}$	$B_{2u}$	$B_{1g}$	XY	$\nu_5^L = 144$	97
$\nu_6^T = 254$	168	$z$	$A_{2u} TO$	$B_{1u}$	$B_{1u}$	$B_{2g}$	ZX	$\nu_6^T = 265$	176
$\nu_6^L = 299$	196	—	$A_{2u} LO$	—	—	—	—	—	—
Sound velocity**[3], $\text{cm/sec} \cdot 10^{-5}$									
$v_{[1\bar{1}0] [110]} = 0.347$			$E_u TA$	$B_{2u}$	$B_{3u}$	$A_g$	$XX, YY, ZZ$	$v_{SM} = 13.6$	8.7
$v_{[1\bar{1}0] [001]} = 1.084$			$A_{2u} TA$	$B_{1u}$	$B_{1u}$	$B_{2g}$	ZX	$v_A = 39$	35
$v_{[1\bar{1}0] [1\bar{1}0]} = 2.08$			$E_u LA$	$B_{2u}$	$B_{2u}$	$B_{1g}$	XY	—	—

\*Single indices—nonzero components of the dipole-moment vector  $M_i$ ; double indices—components of the scattering tensor  $\alpha_{ik}$ . In column 7 are given the selection rules only for the lines that appear at  $T < T_c$ .

\*\*The first and second subscripts represent respectively the propagation direction and the wave polarization.

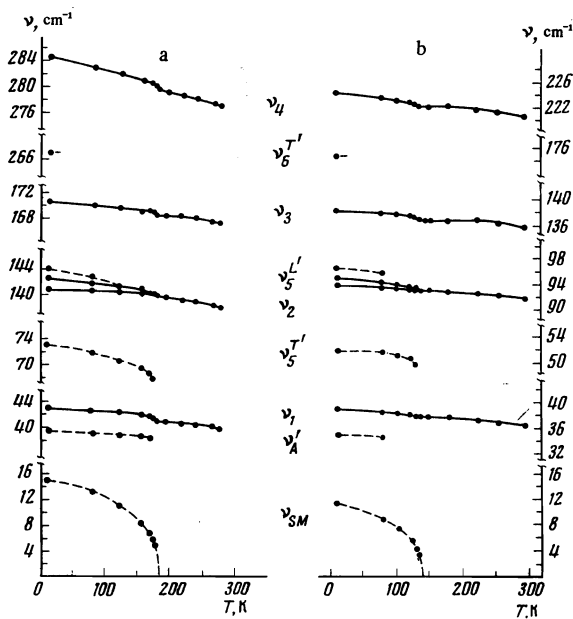


FIG. 2. Temperature dependences of the frequencies of the first-order RS spectra: a)  $\text{Hg}_2\text{Cl}_2$ , b)  $\text{Hg}_2\text{Br}_2$ .

removal of the load.<sup>[8]</sup> In the rhombic domain<sup>[8]</sup> its principal axes are  $X \parallel [1\bar{1}0]$ ,  $Y \parallel [110]$ ,  $Z \parallel [001]$  (Fig. 1), and the scattering tensor is determined in terms of these axes. The depolarization due to the experimental errors did not exceed 7%. The temperature dependence of the RS line intensity was also measured on single-domain uniaxially compressed samples in polarized light.

The results of the investigation of the first-order RS spectra are gathered in Fig. 2. The ordinates represent the spectral intervals in the region of the fundamental frequencies that are active in the RS of tetragonal crystals at  $T > T_c$  (see the table), and also the intervals in which the appearance of new first-order RS lines is observed at  $T < T_c$ . The solid lines show the temperature dependence of the position of the four fundamental frequencies ( $2A_{1g}$  and  $2E_g$ ) observed at  $T > T_c$  in the RS spectra of tetragonal crystals (see the table). When the crystal is cooled from 300°K, a slight short-wave shift of these frequencies takes place. At the point  $T_c$ , all the curves have a distinct anomaly, and the frequency of the doubly degenerate deformation vibration  $\nu_2(E_g)$  is split into a polarized ( $ZX, ZY$ ) doublet whose width increases with further cooling of the crystal below  $T_c$ .

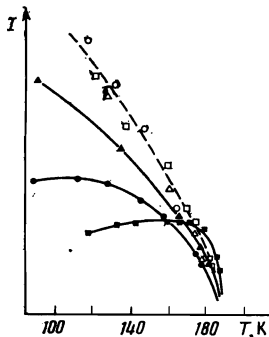


FIG. 3. Temperature dependence of the intensity  $I$  of the  $\text{Hg}_2\text{Cl}_2$  lines: squares— $\nu_{SM}$ , circles— $\nu'_A$ , triangles— $\nu_5^T$ ; the dark and light symbols represent the measured and relative intensities, respectively.

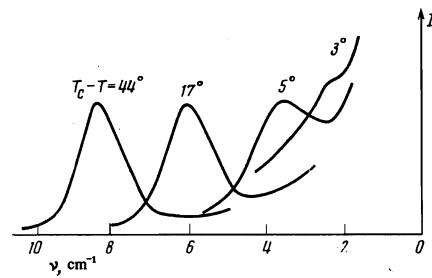


FIG. 4. Line of soft mode in the RS spectra of  $\text{Hg}_2\text{Br}_2$ .

The primes denote the positions of the new first-order lines that appear in the RS spectra at the point  $T = T_c$  and become stronger with further decrease of temperature below  $T_c$ . The new lines are polarized. Altogether we succeeded in observing in the spectra of  $\text{Hg}_2\text{Cl}_2$  and  $\text{Hg}_2\text{Br}_2$  five new lines each, with properties that were analogous in the RS spectra of both crystals.

1. The line  $\nu'_A$  at a distance 2–3  $\text{cm}^{-1}$ , on the long-wave side, from the frequency  $\nu_1$  of the libration  $E_g$  vibration. The line is fully polarized in the off-diagonal component  $ZX$ . Its intensity increases with increasing  $T_c - T$  (Fig. 3).

2. The line  $\nu_5^{T'}$  in the region of the fundamental frequency  $\nu_5^T$  ( $E_u TO$ ), of the vibration active in the IR absorption. The line is observed in diagonal polarization  $YY$ , and its intensity increases with increasing  $T_c - T$  (Fig. 3). A characteristic feature is a relatively large (5–7  $\text{cm}^{-1}$ ) short-wave shift of the line  $\nu_5^{T'}$  when the crystal is cooled from  $T_c$  to 10°K (Fig. 2).

3. The line  $\nu_5^{L'}$  in the region in which are located the frequency  $\nu_2$  of the deformation  $E_g$  vibration and the frequency  $\nu_5^L$  of the longitudinal  $E_u LO$  vibration. The very-low-intensity line  $\nu_5^{L'}$  is superimposed on the short-wave slope of the  $\nu_2$  ( $E_g$ ) line and it can be reliably separated in the spectra only in polarized light. The polarization of  $\nu_5^{L'}$  corresponds to  $XY$ .

4. The line  $\nu_6^{T'}$  in the vicinity of the frequency  $\nu_6^T$  of the transverse  $A_{2u} TO$  vibration active in the IR spectrum. The line has an off-diagonal polarization  $ZX$  and is very weak (it is observed only when cooled to 10°K, so that the second-order RS spectrum is frozen out<sup>[8]</sup>).

5. The line  $\nu_{SM}$  in the low-frequency region of the spectrum is the most important line of the additional SR spectrum that appears at  $T \leq T_c$  (Fig. 4). The frequency of this line depends extraordinarily strongly on the temperature: As  $T \rightarrow T_c^-$  the frequency  $\nu_{SM} \rightarrow 0$ , thus undoubtedly indicating that this line belongs to the soft mode. The line is polarized in diagonal components predominantly in  $YY$ . The line is very narrow, and its half-width ( $\Delta\nu \approx 1.5 \text{ cm}^{-1}$ ) varies little as  $T \rightarrow T_c^-$  (Fig. 4), so that the growth of the damping  $\Delta\nu/\nu_{SM}$  as  $T \rightarrow T_c^-$  is due mainly to the decrease of the frequency  $\nu_{SM}$ . The intensity of the  $\nu_{SM}$  line with increasing  $T_c - T$  first increases rapidly and then, going through a maximum, decreases, thus distinguishing the behavior of this line from the other appearing lines (Fig. 3).

An exceedingly strong dependence of the soft mode in

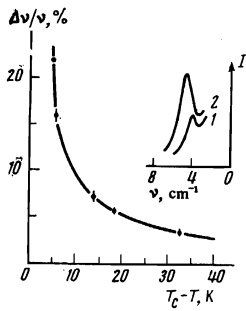


FIG. 5. Temperature dependence of the relative frequency shift of the soft mode of  $\text{Hg}_2\text{Br}_2$  under uniaxial compression ( $\sigma_{[110]} = 0.34 \text{ kg/mm}^2$ ). Insert—spectrum of soft mode in the free crystal (1) and in the crystal stressed at  $\sigma = 0.5 \text{ kg/mm}^2$  (2) at  $T_c - T = 5^\circ$ .

the RS spectrum on the uniaxial compression stress of one-domain samples along the  $[110]$  axis was observed. The deformation noticeably increases the frequency and intensity of the  $\nu_{SM}$  line (Fig. 5). The effect is larger the closer the sample temperature is to  $T_c$ . Figure 5 shows the dependence of the relative deformation line shift  $[\nu_{SM}(\sigma) - \nu_{SM}(0)]/\nu_{SM}(0)$  on  $T_c - T$ . We succeeded in observing a more than 30% relative increase of the soft mode frequency (at  $T_c - T = 5^\circ \text{K}$  and at a stress  $\sigma = 0.5 \text{ kg/mm}^2$ —insert of Fig. 5).

The effective appearance of new lines in the SR spectra of the crystals following the phase transition was first correctly explained<sup>[10]</sup> in a study of similar phenomena in the RS spectra of  $\text{SrTiO}_3$  (structural phase transition at  $T_c = 110^\circ \text{K}$ ). The increase in the number of fundamental vibrations which appears in the first-order RS spectra at  $T \leq T_c$  points to a doubling of the number of molecules in the cell following the transition. A similar transition is induced by the soft mode corresponding to the lattice vibration at the boundary of the Brillouin zone (BZ). As a result, at  $T \leq T_c$  the BZ instability point shifts to the center (the  $\Gamma$  point) of a new low-temperature phase, with half the volume of the BZ, and consequently, the vibrations from this point become active at  $T \leq T_c$  in first-order processes.

On the basis of this idea and the experimentally observed properties of the RS spectra at  $T \leq T_c$  it becomes possible to propose a concrete model of the phase transition, explaining all the known experimental data on the phase transition in  $\text{Hg}_2\text{X}_2$ .

## 2. PHENOMENOLOGICAL THEORY OF STRUCTURAL PHASE TRANSITION IN $\text{Hg}_2\text{X}_2$

### A. Model of transition and Landau thermodynamic potential

The body-centered tetragonal (BCT) lattice corresponding to the  $\text{Hg}_2\text{X}_2$  structure at  $T > T_c$  has in the  $(x, y, z)$  frame the basis vectors

$$\mathbf{a}_1 \left( \frac{a}{2}, -\frac{a}{2}, \frac{c}{2} \right), \quad \mathbf{a}_2 \left( -\frac{a}{2}, \frac{a}{2}, \frac{c}{2} \right), \quad \mathbf{a}_3 \left( \frac{a}{2}, \frac{a}{2}, -\frac{c}{2} \right), \quad (1)$$

where  $a$  and  $c$  are the parameters of the unit cell (Fig. 6a). The reciprocal lattice vectors are

$$\mathbf{b}_1 \left( \frac{1}{a}, 0, \frac{1}{c} \right), \quad \mathbf{b}_2 \left( 0, \frac{1}{a}, \frac{1}{c} \right), \quad \mathbf{b}_3 \left( \frac{1}{a}, \frac{1}{a}, 0 \right). \quad (2)$$

The first Brillouin zone of the BCT lattice, shown in Fig. 6b by the solid line, has singular points on its boundary, namely  $Z(0, 0, 1/c)$  and the two nonequivalent  $X$  points  $X_1(1/2a, 1/2a, 0)$  and  $X_2(1/2a, -1/2a, 0)$ .

According to our concepts the transition is induced by phonon instability at the  $X$  points of the Brillouin zone of the BCT lattice at  $T \leq T_c$ . The low frequency of the observed soft mode ( $\nu_{SM}^{\text{max}} \sim 10 - 15 \text{ cm}^{-1}$ ) attests to the fact that the corresponding vibration is connected with the acoustic mode of lowest energy in the elastic spectrum of  $\text{Hg}_2\text{X}_2$ . This mode, judging from acoustic measurements,<sup>[3]</sup> is the transverse  $TA$  mode with displacements of the atoms in the basal plane of the crystal.

We consider two non-equivalent points on the Brillouin-zone boundary of the BCT lattice,  $X_1$  and  $X_2$ , with coordinates  $\mathbf{K}(X_1) = \frac{1}{2}\mathbf{b}_3$  and  $\mathbf{K}(X_2) = \frac{1}{2}(\mathbf{b}_2 - \mathbf{b}_1)$ . The vectors  $\mathbf{K}(X_1)$  and  $\mathbf{K}(X_2)$  form a star of the irreducible representation of the tetragonal group of the crystal  $D_{4h}$ . The point group of the wave vector  $\mathbf{K}(X_1)$  corresponds to  $D_{2h}$ . The acoustic transverse displacements in the basal plane at the points  $X_1$  and  $X_2$  correspond respectively to the representations  $B_{3u}$  and  $B_{2u}$  of the group of the wave vector  $D_{2h}$ .

The eigenvectors of the representations  $B_{3u}[\mathbf{K}(X_1)]$  and  $B_{2u}[\mathbf{K}(X_2)]$

$$\varphi_1 = \exp[-2i\pi\mathbf{K}(X_1)\mathbf{r}] \psi_{B_{3u}}(\mathbf{r}), \quad \varphi_2 = \exp[-2i\pi\mathbf{K}(X_2)\mathbf{r}] \psi_{B_{2u}}(\mathbf{r}) \quad (3)$$

form a basis of a two-dimensional irreducible representation  $\tau$  of the space group of the crystal  $D_{4h}^{17}$ .<sup>[11]</sup>

The representation  $\tau$  is active in the induction of the phase transition, since  $[\tau]^3$  does not contain a unit representation, and  $\{\tau\}^2$ , which does not contain a null-star, has no common representations with the vector representation. Inasmuch as the representation  $\tau$  is two-dimensional, the transition parameter remains two-component. The electron density in the crystal will be expressed in the form

$$\rho(\mathbf{r}) = \rho_0 + c_1\varphi_1 + c_2\varphi_2, \quad (4)$$

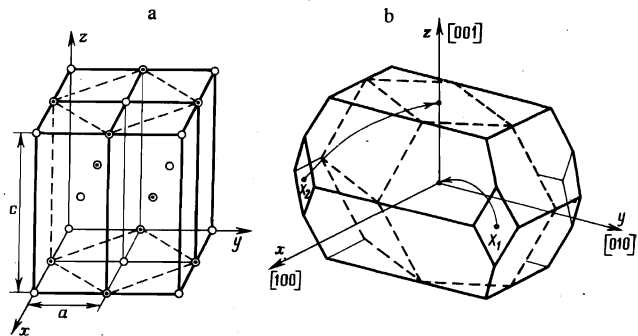


FIG. 6. Bravais lattice (a) and Brillouin zone (b) of  $\text{Hg}_2\text{X}_2$  crystals in the tetragonal and orthorhombic phases. The Bravais lattice points which are not congruent at  $T \leq T_c$  are differently designated.

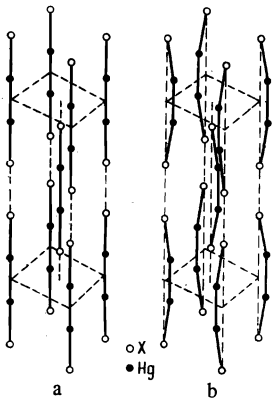


FIG. 7. Atomic displacements in  $\text{Hg}_2\text{X}_2$  following the structural phase transition  $D_{4h}^{17}$  (a)  $\rightarrow D_{2h}^{17}$  (b).

where  $\rho_0$  is the density in the tetragonal crystal and  $c_1$  and  $c_2$  are the parameters of the transition (displacement), which transform like  $\varphi_1$  and  $\varphi_2$ .

We consider the product  $[\tau]^2$ . Since the point group of the vectors  $\mathbf{K}_i - \mathbf{K}_j$  ( $i, j = 1, 2$ ) corresponds to  $D_{4h}$  ( $2\mathbf{K}_1$  and  $2\mathbf{K}_2$  are equivalent to  $\mathbf{K} = 0$ , and the vector  $\mathbf{K}_1 + \mathbf{K}_2$  is equivalent to  $\mathbf{K}(Z)$ ), the expansion of  $[\tau]^2$  in the irreducible representations of the group  $D_{4h}^{17}$  takes the form

$$[\tau]^2 = A_{1g}(\Gamma) + B_{2g}(\Gamma) + B_{1g}(Z), \quad (5)$$

where  $A_{1g}$ ,  $B_{1g}$ ,  $B_{2g}$  are the representations of the point group  $D_{4h}$ , and the parentheses of (5) contain the corresponding points at the center ( $\Gamma$ ) and the boundary ( $Z$ ) of the Brillouin zone.

The eigenvectors of these representations and the corresponding transition parameters are given by

$$\begin{aligned} A_{1g}: & \quad x^2 + y^2, \quad z^2; & c_1^2 + c_2^2 \\ B_{2g}: & \quad xy; & c_1^2 - c_2^2. \\ B_{1g}(Z): & \quad -, & c_1 c_2. \end{aligned} \quad (6)$$

Expanding the specific (per molecule of  $\text{Hg}_2\text{X}_2$ ) thermodynamic potential  $\Phi(c_1, c_2)$  in terms of invariants made up of components of the displacement parameter and of the strain tensor  $\varepsilon_i$  in the Voigt notation,<sup>4)</sup> we obtain

$$\begin{aligned} \Phi = & \frac{1}{2}\alpha(c_1^2 + c_2^2) + \frac{1}{4}\beta_1(c_1^2 - c_2^2)^2 + \frac{1}{4}\beta_2(2c_1 c_2)^2 \\ & + \frac{1}{2}B(c_1^2 - c_2^2)\varepsilon_6 + \frac{1}{2}D(c_1^2 + c_2^2)(\varepsilon_1 + \varepsilon_2 - 2\varepsilon_3) \\ & + \frac{1}{2}F(c_1^2 + c_2^2)(\varepsilon_1 + \varepsilon_2 + \varepsilon_3) + \left(\frac{1}{2} \sum_{ij} c_{ij}\varepsilon_i\varepsilon_j - \sum_i \sigma_i\varepsilon_i\right)v, \end{aligned} \quad (7)$$

where  $c_{ij}$  are the elastic constants,  $\sigma_i$  is the stress tensor,  $v = \frac{1}{2}a^2c$  is the volume of the unit cell, and  $\alpha$ ,  $\beta_1$ ,  $\beta_2$ ,  $B$ ,  $F$ ,  $D$  are the parameters of the potential and are functions of the temperature.

Using the conditions for the minimum of the thermodynamic potential  $\partial\Phi/\partial\varepsilon_i = 0$  and changing over to new variables

$$\rho^2 = c_1^2 + c_2^2, \quad \varphi = \arctg[(c_1 - c_2)/(c_1 + c_2)],$$

we rewrite (7) in the form

$$\begin{aligned} \Phi = & \frac{1}{2}\alpha\rho^2 + \frac{1}{4}\rho^4(\gamma_1 \sin^2 2\varphi + \gamma_2 \cos^2 2\varphi) + \frac{1}{2}B\rho^2 \sin 2\varphi \varepsilon_6 \varepsilon_6 \\ & + \frac{1}{2}D\rho^2[(\sigma_1 + \sigma_2)(s_{11} + s_{12} - 2s_{13}) + 2\sigma_3(s_{13} - s_{33})] \\ & + \frac{1}{2}F\rho^2[(\sigma_1 + \sigma_2)(s_{11} + s_{12} + s_{33}) + \sigma_3(2s_{13} + s_{33})] - \frac{1}{2}v \sum_{ij} s_{ij}\sigma_i\sigma_j, \end{aligned} \quad (8)$$

where  $S_{ij}$  are the elastic moduli and

$$\gamma_1 = \beta_1 - \frac{1}{2v}B^2 s_{66} - \frac{\Pi}{v}, \quad \gamma_2 = \beta_2 - \frac{\Pi}{v},$$

$$\Pi = D^2(s_{11} + s_{12} - 4s_{13} + 2s_{33}) + 2FD(s_{11} + s_{12} - s_{13} - s_{33}) + F^2(s_{11} + s_{12} + 3s_{13} + s_{33}). \quad (9)$$

We examine the potential  $\Phi$  (8) of the  $\text{Hg}_2\text{X}_2$  crystals in the absence of external stresses:  $\sigma_i = 0$ . The minimum conditions are of the form

$$\frac{\partial\Phi}{\partial\rho} = \rho[\alpha + \rho^2(\gamma_1 \sin^2 2\varphi + \gamma_2 \cos^2 2\varphi)] = 0, \quad (10)$$

$$\frac{\partial\Phi}{\partial\varphi} = \frac{1}{2}\rho^4(\gamma_1 - \gamma_2)\sin 4\varphi = 0, \quad (11)$$

$$\frac{\partial^2\Phi}{\partial\rho^2} > 0, \quad \frac{\partial^2\Phi}{\partial\rho^2} \frac{\partial^2\Phi}{\partial\varphi^2} - \left(\frac{\partial^2\Phi}{\partial\rho\partial\varphi}\right)^2 > 0. \quad (12)$$

The solutions (10) and (11) under the conditions (12) take the form

$$\text{I. } \rho = 0 \text{ if } \alpha > 0; \quad (13)$$

$$\text{II. } \cos 2\varphi = 0, \quad \rho^2 = -\alpha/\gamma_1 \text{ if } \alpha < 0, \quad \gamma_2 > \gamma_1 > 0; \quad (14)$$

$$\text{III. } \sin 2\varphi = 0, \quad \rho^2 = -\alpha/\gamma_2 \text{ if } \alpha < 0, \quad \gamma_1 > \gamma_2 > 0. \quad (15)$$

The solution I, where the components  $c_1$  and  $c_2$  of the transition parameter are equal to zero, obviously corresponds to the high-temperature ( $T > T_c$ ) tetragonal phase. Solutions II and III correspond to two low-temperature phases (II and III), into one of which, depending on the ratio of the parameters  $\gamma_1$  and  $\gamma_2$ , a transition can take place at  $T < T_c$ . Inasmuch as  $\alpha > 0$  at  $T > T_c$  and  $\alpha < 0$  at  $T < T_c$ , we can put  $\alpha = \lambda(T - T_c)$ , where  $\lambda > 0$  is a parameter;  $\alpha$  vanishes at  $T = T_c$ .

## B. Properties of low-temperature orthorhombic phase

In phase III, the transition-parameter components  $c_1$  and  $c_2$ , which can be regarded as projections of the displacement of the molecule  $\text{Hg}_2\text{X}_2$  on the rhombic axes  $X$  and  $Y$ , determine in accordance with (15) four domain types ( $c_1 = \pm c_2 = \pm \rho/\sqrt{2}$ ) with molecules displaced along the tetragonal axes  $\pm x$  and  $\pm y$ . The structural phase transition I  $\rightarrow$  III should have been accompanied by a splitting of the unit-cell volume into four and by spontaneous deformation (at  $T < T_c$ ) along the  $z$  axis, and the symmetry of phase III is tetragonal. The potential (7) admits of no connection between the displacements of the molecules and the shear deformation  $\sigma_6$  in phase III. The indicated characteristics of phase III contradict the experimental data.

In experiment, a transition to the low-temperature phase II is realized (i.e.,  $\gamma_2 > \gamma_1$ ). For this phase, the solution (14) admits of formation of four types of domains, which differ in the orientation of the displacements of the molecules  $\text{Hg}_2\text{X}_2$  in the lattice along the rhombic axes:

- 1)  $c_1 = \rho, c_2 = 0$  ( $\varphi = \pi/4$ );
- 2)  $c_1 = -\rho, c_2 = 0$  ( $\varphi = 5\pi/4$ );
- 3)  $c_1 = 0, c_2 = \rho$  ( $\varphi = 7\pi/4$ );
- 4)  $c_1 = 0, c_2 = -\rho$  ( $\varphi = 3\pi/4$ ).

Figure 7b shows schematically the displacements in

the individual domain 1). Two parallel shifts of the centers of gravity of the molecules  $\text{Hg}_2\text{X}_2$  take place here along the  $[\bar{1}\bar{1}0]$  directions,<sup>5)</sup> and the directions of the shifts are opposite in neighboring atomic planes (110). The domains 2) differ from 1) only in the signs of the shifts that occur in the same systems of (110) planes. In domains 3) and 4) the corresponding displacements occur in a perpendicular system of  $(\bar{1}\bar{1}0)$  planes.

The structure of the domain of phase II (Fig. 7b) is thus the result of the "freezing," at  $T < T_c$ , of the displacements of the molecules in the transverse acoustic wave with wave vector in one of the  $X$  points of the Brillouin zone of the BCT lattice and with polarization in the (001) plane. A simple analysis of the geometry of this structure shows that the positional symmetry of the  $\text{Hg}_2\text{X}_2$  molecule is lowered by the transition from the tetragonal  $D_{4h}$  to the orthorhombic  $C_{2v}$ , and the point symmetry of the entire crystal is lowered from  $D_{4h}$  to  $D_{2h}$ . The molecules in the neighboring (110) planes (the domains 1) and 2)) become non-congruent and the number of molecules per cell doubles. The dashed lines in Fig. 6a delineate the new orthorhombic cell (they join the molecules that remain congruent); this cell corresponds to a base-centered orthorhombic lattice. The principal axes,  $Z$ ,  $X$ ,  $Y$  of the orthorhombic axis are directed along the previous axis of the tetragonal crystal  $[001]$ ,  $[\bar{1}\bar{1}0]$ , and  $[110]$ . The conclusions with respect to the structure follow also rigorously mathematically from the condition that the plane  $p(\mathbf{r})$  (4) at  $c_1 = 0$  or  $c_2 = 0$  is invariant to the corresponding symmetry transformations. These transformations identify the space group of the low-temperature phase II as  $D_{2h}^1$ .

The basis vectors of the base-centered orthorhombic lattice, in the coordinate system connected with the rhombic axis  $X = (x - y)/\sqrt{2}$ ,  $Y = (x + y)/\sqrt{2}$ ,  $Z = z$ , are given by (Fig. 6)

$$\mathbf{a}'_1 = (0, 2\tau_y, 0), \quad \mathbf{a}'_2 = (\tau_x, 0, \tau_z), \quad \mathbf{a}'_3 = (-\tau_x, 0, \tau_z), \quad (16)$$

where

$$\tau_x = (1 - \varepsilon_3^0 + \varepsilon_3^0) a / \sqrt{2}, \quad \tau_y = (1 + \varepsilon_3^0 + \varepsilon_3^0) a / \sqrt{2} \\ \tau_z = (1 + \varepsilon_3^0) c / 2;$$

$\varepsilon_1^0, \varepsilon_3^0, \varepsilon_6^0$  are the components of the spontaneous stress tensor produced at  $T \leq T_c$ . The stresses obtain from the condition that  $\Phi$  be a minimum at  $T \leq T_c$ :

$$\varepsilon_1^0 = \varepsilon_2^0 = \frac{\lambda(T - T_c)}{2\gamma_{1\nu}} [(s_{11} + s_{12})(F + D) + s_{13}(F - 2D)], \quad (17)$$

$$\varepsilon_3^0 = \frac{\lambda(T - T_c)}{2\gamma_{1\nu}} [2s_{33}(F + D) + s_{36}(F - 2D)], \quad (18)$$

$$\varepsilon_6^0 = \frac{\lambda B(T - T_c)}{2\gamma_{1\nu}} s_{66} \sin 2\varphi. \quad (19)$$

It follows from (17)–(19) that the spontaneous stress  $\varepsilon_i^0$  is the same in domains 1) and 2) ( $\sin 2\varphi = +1$ ); for the other pair of domains, 3) and 4), the sign of  $\varepsilon_6^0$  is opposite ( $\sin 2\varphi = -1$ ) and is also the same for the two domains. Consequently the domains 1) and 2) do not differ from each other in any way with respect to their macroscopic properties. The same pertains to the pair 3)

and 4) ("antiphase domains"<sup>[12]</sup>). The domain pairs 1), 2) have a different "orientation" of the spontaneous strain and other macroscopic properties than the domain 3), 4). In particular, optical birefringence should take place in the  $xy$  plane, while the indicatrix axes are parallel to  $[110]$  and  $[\bar{1}\bar{1}0]$  and differ in a rotation through  $90^\circ$  for the two pairs of domains. From the condition that the medium be continuous at the domain boundaries it follows that the domains 1), 2), and 3), 4) are separated by boundaries inclined  $45^\circ$  to the rhombic axis, i. e., directed along  $[100]$  and  $[010]$ .

At the transition point, jumpwise changes take place in the heat capacity of the crystal

$$\Delta C_p = \lambda^2 T_c / 2\gamma_{1\nu} \quad (20)$$

and in the elastic constants  $c_{ij}$ . The jumps of the elastic constants  $\Delta c_{ij} = c_{ij}|_{T_c} - c_{ij}|_{T < T_c}$  are equal to

$$\Delta c_{11} = \Delta c_{22} = \Delta c_{12} = -\frac{(F+D)^2}{2\gamma_{1\nu}}, \quad \Delta c_{33} = -\frac{(F-2D)^2}{2\gamma_{1\nu}}, \\ \Delta c_{13} = \Delta c_{23} = -\frac{(F+D)(F-2D)}{2\gamma_{1\nu}}, \quad \Delta c_{36} = -\frac{(F-2D)B \sin 2\varphi}{2\gamma_{1\nu}}, \quad (21) \\ \Delta c_{16} = \Delta c_{26} = -\frac{(F+D)B \sin 2\varphi}{2\gamma_{1\nu}}, \quad \Delta c_{66} = -\frac{B^2}{2\gamma_{1\nu}}.$$

We consider now a transition in the presence of external stresses and confine ourselves to the most important case, when the stress  $\sigma_6$  differs from zero and all other  $\sigma_i (i \neq 6) = 0$ . The displacement parameter in phase II is defined by the equation

$$\rho^2 = -[\lambda(T - T_c) + B s_{66} \sigma_6 \sin 2\varphi] / \gamma_{1\nu}, \quad \cos 2\varphi = 0, \quad (22)$$

which determines the dependence of  $T_c$  on the external stress:

$$\Delta T_c = -B \lambda^{-1} s_{66} \sigma_6 \sin 2\varphi. \quad (23)$$

For domains that differ in the sign of  $\sin 2\varphi$ , the temperature  $T_c$ , the displacement parameter  $\rho$ , and the frequency of the soft mode at  $\sigma_6 > 0$ , if  $B > 0$ , increase ( $\sin 2\varphi = -1$ ,  $\Delta T_c > 0$ ), or else decrease ( $\sin 2\varphi = +1$ ,  $\Delta T_c < 0$ ). The condition  $\partial^2 \Phi / \partial \varphi^2 > 0$  for the stable equilibrium of the domains with  $\Delta T_c > 0$  is satisfied at all stresses  $\sigma_6$ . At the same time, domains with  $\Delta T_c < 0$  become unstable ( $\partial^2 \Phi / \partial \varphi^2 = 0$ ) at a stress

$$|\sigma_6^0| = \frac{\lambda(T_c - T) c_{66}}{|B|} \left(1 - \frac{\gamma_1}{\gamma_2}\right). \quad (24)$$

Thus, if  $B > 0$ , only the antiphase domain 3) and 4) with  $\sin 2\varphi = -1$  remain in the crystal at  $\sigma_6 > \sigma_6^0$ ; this corresponds macroscopically to the crystal becoming single-domain.

### C. Influence of phase transition on the optical spectra

The solution II (14) for the individual domains yields a zero value for one of the two components of the transition parameter,  $c_1$  or  $c_2$ . This means, with (3) and (4) taken into account, that the transition is due to the instability of the acoustic vibrations in one of the  $X$  points. Let this be the vibration  $B_{3u}$  at the point  $X_1$  (the

domain of Fig. 7b). We then have for the vibration frequency of the acoustic soft modes at  $X_1$  and  $X_2$  near the transition temperature<sup>[12]</sup>

$$\omega^2[\mathbf{K}(X_1)] = \frac{1}{M} \frac{\partial^2 \Phi}{\partial \rho^2} = \begin{cases} \lambda(T-T_c)/M, & T > T_c \\ 2\lambda(T_c-T)/M, & T < T_c \end{cases} \quad (25)$$

$$\omega^2[\mathbf{K}(X_2)] = \frac{1}{M\rho^2} \frac{\partial^2 \Phi}{\partial \varphi^2} = \begin{cases} \lambda(T-T_c)/M, & T > T_c \\ \frac{2\lambda}{M}(T_c-T) \left( \frac{\gamma_2}{\gamma_1} - 1 \right), & T < T_c \end{cases} \quad (26)$$

where  $M$  is the mass of the  $\text{Hg}_2\text{X}_2$  molecule.

At  $T > T_c$ , the vibrations at the points  $X_1$  and  $X_2$  are doubly degenerate. At  $T < T_c$ , the degeneracy is lifted, since  $X_1$  and  $X_2$  goes over into different points of the Brillouin zone of the low-temperature base-centered orthorhombic lattice. For this lattice, the reciprocal vectors are given by

$$\mathbf{b}'_1 = \mathbf{b}_1 - \frac{1}{2}\mathbf{b}_3, \quad \mathbf{b}'_2 = \frac{1}{2}\mathbf{b}_3, \quad \mathbf{b}'_3 = \mathbf{b}_2 - \frac{1}{2}\mathbf{b}_1; \quad (27)$$

its Brillouin zone is shown by the dashed line in Fig. 6b. It is seen that  $X_1(\mathbf{b}_3/2)$  corresponds to the reciprocal vector  $\mathbf{b}'_2$  and consequently goes over to the center (the  $\Gamma$  point) of the Brillouin zone of the orthorhombic lattice. The point  $X_2(\frac{1}{2}(\mathbf{b}_2 - \mathbf{b}_1))$  lands on the boundary of the new Brillouin zone at the point  $Z$ .

The  $X_1 \rightarrow \Gamma$  jump causes all the vibrations at  $X_1$  which were not optically active at  $T > T_c$ , including the soft mode  $\omega_{SM}$ , to become optically active in first order at  $T \leq T_c$ . The selection rules for the new fundamental vibrations at  $T \leq T_c$  can be easily obtained with the aid of group theory: by analyzing the symmetry transformations of the vibrations at  $X_1$  in the  $X_1 \rightarrow \Gamma$  jump, or else by direct derivation of the symmetry of the fundamental vibrations of the crystal  $D_{2h}^{17}$  with two  $\text{Hg}_2\text{X}_2$  molecules per cell, having positional symmetry  $C_{2v}$  (by the method described in<sup>[13]</sup>). The table lists the results of the calculations for the vibrations of all the branches of the elastic spectrum of the tetragonal crystal  $\text{Hg}_2\text{X}_2$  at the  $X$  point, which go over at  $T \leq T_c$  to the  $\Gamma$  point of the orthorhombic crystal. Column 4 indicates the symmetry of the branches of the point  $X$  for a tetragonal crystal. In the right-hand part of the table (columns 5-8) are given the data for the orthorhombic crystal  $D_{2h}^{17}$ . Column 5 lists the symmetry of the fundamental vibrations of the point  $\Gamma$  ( $D_{2h}$ ), coming from the fundamental vibrations of the tetragonal crystal at the point  $\Gamma$  ( $D_{4h}$ ) (column 3). The main effect of the  $D_{4h} \rightarrow D_{2h}$  transition at the  $\Gamma$  point is the doublet splitting of the doubly degenerate  $E_g$  vibrations. In column 6 is indicated the symmetry of the point  $\Gamma$  ( $D_{2h}$ ) of the vibrations resulting from vibrations at the  $X_1$  point of the Brillouin zone (column 4) of the tetragonal crystal. For these new fundamental frequencies, column 7 lists the selection rules in the IR and RS spectra. It is seen that in the RS spectrum at  $T \leq T_c$  there can appear vibrations from the point  $X$  of all the "odd" branches of the spectrum of the tetragonal crystal—three optical branches and three acoustic branches. The vibrations of the "even" branches at  $X$  can yield new lines in the IR spectra of the orthorhombic phase.

It follows from general considerations that at  $T < T_c$  the splitting of the fundamental  $E_g$  vibrations, just as the intensity  $I_0$  of the lines of the RS spectrum from the  $X$  point, is proportional to the square of the displacement parameter  $\rho$ . In the Landau-theory approximation we have  $I_0 \propto \rho^2 \propto (T_c - T)$ . Therefore the intensity of the Stoke's lines of the developing RS spectrum is

$$I_s \sim I_0(T) [n(T) + 1], \quad (28)$$

where  $n(T) = [\exp(\hbar\omega/kT) - 1]^{-1}$  is the usual temperature characterizing the population of the vibrational modes.

### 3. COMPARISON OF EXPERIMENTAL RESULTS WITH CALCULATION

The calculated data in the table account well for the experimental results on the RS spectra at  $T \leq T_c$  (Sec. 1). In particular, they explain the observed polarized splitting of the degenerate frequency of the deformation vibration  $\nu_2(E_g)$  in the transition  $D_{4h} \rightarrow D_{2h}$  ( $E_g = B_{2g} + B_{3g}$ ). The absence of an analogous splitting in the other degenerate librational vibration  $\nu_1(E_g)$  is more readily due to the smallness of this splitting (it is estimated that  $\sim 0.3 \text{ cm}^{-1}$ , if it is assumed that the relative splitting of  $\nu_1$  is  $\sim 1\%$  as that of  $\nu_2$ ).

The theory (columns 6 and 7 of the table) explains also the properties of the new lines that appear in the RS spectrum at  $T \leq T_c$  and correspond to the fundamental vibrations of the  $D_{2h}^{17}$  phase, coming from the  $X$  point of the  $D_{4h}^{17}$  crystal. The experimental frequencies of the new lines are given in column 8. Experiment has revealed five new lines out of the six theoretically possible. The line positions and polarizations agree with the calculation. The frequencies of the three optical branches  $\nu_5^{T'}$ ,  $\nu_5^{L'}$ ,  $\nu_6^{T'}$  which appear in the RS spectrum from the  $X$  point (column 8) are close to the fundamental frequencies of the corresponding branches  $E_u TO$ ,  $E_u LO$ ,  $A_{2u} TO$ , known from the IR spectra (column 1). This points to a small dispersion of the intramolecular dipole vibrations (an exact comparison of the frequencies is made difficult here by the fact that the IR spectra<sup>[5]</sup> and the RS spectra were measured at different temperatures).

Vibrations ( $\nu_{SM}$  and  $\nu'_A$ ) from the  $X$  point of two transverse acoustic branches appear in the RS spectra also at  $T \leq T_c$ ; one of them is a soft mode. The values of  $\nu_{SM}$  and  $\nu'_A$  agree with the estimates of the frequencies of these modes at the  $X$  point, carried out for  $\text{Hg}_2\text{Cl}_2$  in the Debye approximation on the basis of the known (column 1) sound velocities:

$$\nu_{TA}(B_{3u}) = \nu_{(110)}^{(110)} \frac{q_x}{c} = 18 \text{ cm}^{-1}, \quad \nu_{TA}(B_{1u}) = \nu_{(110)}^{(001)} \frac{q_x}{c} = 54 \text{ cm}^{-1},$$

where  $q_x = (\sqrt{2}a)^{-1}$  is the reciprocal wavelength of the phonon at the  $X$  point ( $a \approx 4.5 \text{ \AA}$ ), and  $c$  is the speed of light. As expected, owing to the dispersion of the acoustic branches, the experimental frequencies are lower than the Debye frequencies. The  $\nu_{SM}$  and  $\nu'_A$  vibrations at  $T \leq T_c$  are obviously of the translational type. It is seen from column 6 of the table that the soft mode  $\nu_{SM}$  is fully symmetrical ( $A_g$ ) at  $T \leq T_c$ , as is also

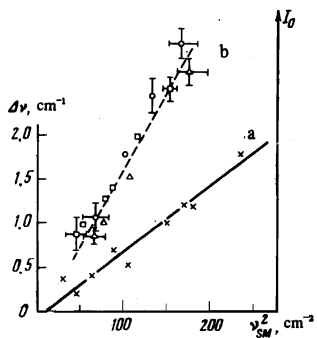


FIG. 8. a) Width of the doublet  $\nu_2(E_g)$  and b) relative intensity  $I_0$  of the produced lines at  $T \leq T_c$ , as functions of  $\nu_{SM}^2$  (the experimental points correspond to Fig. 3) ( $\text{Hg}_2\text{Cl}_2$ ).

the opposite  $\nu_5^{T'}$  vibration connected with the  $E_u TO$  branch. Since they have the same symmetry, these vibrations interact with each other. This explains the appreciable decrease of the frequency of  $\nu_5^{T'}$  as  $T \rightarrow T_c^-$  (Fig. 2). It is due to the interaction of  $\nu_5^{T'}$  with the soft mode, whose frequency  $\nu_{SM} \rightarrow 0$ .

The detailed agreement between the experimental and calculated data on the RS spectra offers convincing evidence in favor of the transition model used in Sec. 2. The consequences of this model, described in Sec. 2, explain also all the other known experimental facts concerning the orthorhombic macrosymmetry of the phase (with inversion center), the directions of the optical axes in it, the orientation of the domain walls, and the ferroelastic properties.<sup>[6]</sup> The space group of the low-temperature phase  $D_{2h}^{17}$ , obtained on the basis of an analysis of purely spectroscopic data, is confirmed by direct x-ray structure measurements of  $\text{Hg}_2\text{Cl}_2$  at low temperatures.<sup>[6]</sup>

We note also that a microscopic harmonic-approximation calculation of the vibrational spectrum of  $\text{Hg}_2\text{Cl}_2$  at the X point on the basis of the data for the  $\Gamma$  point (elastic and dielectric constants, fundamental frequencies), has yielded for the frequency of the transverse acoustic branch in X an imaginary value, which also attests to the instability of the mode.<sup>[14]</sup>

It is of interest to compare quantitatively the experimental results with the conclusions of the Landau phenomenological theory (Sec. 2). This comparison is hindered to some extent by the fact that the main temperature dependences of this theory,  $\rho^2 \propto T_c - T$  and  $\nu_{SM}^2 \propto T_c - T$  near  $T_c$  are usually not satisfied, owing to correlation effects and to the large fluctuations of  $\rho$  and  $\varphi$ .<sup>[12]</sup> Although no precision measurements of  $\nu_{SM}(T)$  were made for  $\text{Hg}_2\text{X}_2$ , within the limits of experimental accuracy the obtained curves (Fig. 2) are definitely in better agreement with the relation  $\nu_{SM}^2 \propto T_c - T$  in a certain vicinity of  $T_c$ . A relation of this type was established earlier, for example, for the structural phase transition in  $\text{SrTiO}_3$ .<sup>[15]</sup> In<sup>[15]</sup> it was shown also, with  $\text{SrTiO}_3$  as an example, that the proportionality  $\rho^2(T) \propto \nu_{SM}^2(T)$  is satisfied in experiment in a sufficiently wide range of  $T_c - T$ , although the functions  $\rho^2(T)$  and  $\nu_{SM}^2(T)$ , when taken separately, deviate significantly from those predicted by the Landau theory. This circum-

stance allows us to use for  $\text{Hg}_2\text{X}_2$  the experimentally obtained values of  $\nu_{SM}(T)$  as an argument when checking on the theoretical dependences of various quantities on the (unknown) displacement parameter  $\rho(T)$ .

In Fig. 8 (curve a), the experimental width of the doublet splitting at  $T \leq T_c$  of the frequency  $\nu_2$  of the deformation vibration  $E_g (= B_{2g} + B_{3g})$  is plotted as a function of  $\nu_{SM}^2$ . A linear relation is obtained, as predicted by the theory ( $\Delta \propto \rho^2$ —see Sec. 2). In the analysis of the intensities of the produced SR spectral lines we must start from values of  $I$  in which account is taken of the population of the phonon modes  $n(T)$  (28). Figure 3 shows the normalized "relative" values of  $I_0(T)$  obtained for the frequencies  $\nu_{SM}$ ,  $\nu_A'$ , and  $\nu_5^{T'}$  from the experimental values of  $I_S(T)$  with allowance for the quantity  $n(T+1)$  (for the soft mode  $\nu_{SM}$  the quantity  $n(T)$  takes into account the temperature shift of the frequency. It is seen that the temperature dependences of the intensity for the different lines is practically the same and is described by a universal  $I_0(T)$  curve (shown dashed in Fig. 3). Figure 8 shows the  $I_0(T)$  curve of Fig. 3, recalculated in terms of the function  $\nu_{SM}(T)$  into the function  $I_0(\nu_{SM}^2)$ , which is linear (curve b) as follows from the theory ( $I_0 \propto \rho^2$ ).

For  $\text{Hg}_2\text{Cl}_2$ , the parameters of the thermodynamic potential (8) were estimated from the comparison of the experimental data with four theoretical dependences:

- The temperature dependence of the frequency of the soft mode  $\nu_{SM}$  (25) determines the value of  $\lambda$ . The experimental values were taken for the interval  $0.68 < T/T_c < 0.88$ , where  $\nu_{SM}^2(T)$  is approximately linear. In (25) we have  $M = 472$  a. u. (the mass of the  $\text{Hg}_2\text{Cl}_2$  molecule).
- The dependence of the temperature shift  $\Delta T_c$  of the transition on the uniaxial compression stress  $\sigma_6$  (23) yields the value of  $B$ . The shift  $\Delta T_c$  is determined from the experimental shift of the frequency of the soft mode following a compression  $\sigma_{[110]}$  ( $\sigma_6 = -\frac{1}{2}\sigma_{[110]}$ )—Fig. 5; the value of  $d\nu_{SM}^2/d\sigma_{[110]}$  was considered in the region  $0.68 < T/T_c < 0.88$ .
- The spontaneous deformation  $\epsilon_6^0$  (19) in the low-temperature phase was used to determine  $\gamma_1$ . From the preliminary x-ray structure measurements of the orthorhombic lattice constants at  $T = 125^\circ\text{K}$ , a value  $\epsilon_6^0 \approx 0.1\%$  was obtained from formula (16).
- The monodomainization stress  $\sigma_6^0$  (24) yields an estimate of the ratio  $\gamma_1/\gamma_2$ . The value of  $\sigma_6^0$  was obtained from experiment on the monodomainization of multidomain samples by compression along [110].<sup>[6]</sup> Since the influence of the domain walls and the presence of structure defects can greatly lower the real stress, it can be assumed that  $\sigma_6^0 > \sigma_{exp}$  where  $\sigma_{exp} = 10 \text{ kg/cm}^2$  is the observed threshold monodomainization stress<sup>[6]</sup> at  $T = 77^\circ\text{K}$ .

In this manner, under the assumption that  $F = D = 0$ , and using  $c_{66} = 12.25 \times 10^{10} \text{ dyn/cm}^2$ ,<sup>[3]</sup> we obtained the four constants of the potential (8):

$$\lambda = 38 \text{ erg/cm}^2\text{K}, \quad |B| = 3 \cdot 10^5 \text{ erg/cm}^2$$

$$\gamma_1 = 2.4 \cdot 10^{22} \text{ erg/cm}^4, \quad 1 - \gamma_1/\gamma_2 > 0.0060.$$

From these values we can estimate the heat-capacity jumps (20)  $\Delta C_p = 0.08 \text{ cal/mole-K}$  and of the elastic constant (21) expected in the transition (the largest jump, amounting to  $\sim 15\%$ , is  $\Delta C_{66} = 1.7 \times 10^{10} \text{ dyn/cm}^2$ ).

We note in conclusion that  $\text{Hg}_2\text{Cl}_2$  and  $\text{Hg}_2\text{Br}_2$  are pure extrinsic ferroelastics with a two-component transition parameter connected with the soft mode at the point  $X$  on the Brillouin-zone boundary. It is important to note that the double degeneracy of the soft mode at  $T > T_c$  is due to the existence of two nonequivalent points  $X$  on the boundary of the zone. This distinguishes the case of  $\text{Hg}_2\text{X}_2$  from the classical case of the  $110^\circ\text{K}$  transition in  $\text{SrTiO}_3$ , where the fact that the transition parameter is not one-dimensional is due to the (triple) degeneracy of the intrinsic oscillation at one point ( $R$ ) of the Brillouin zone.

The simplicity of the crystallographic structure and of the fundamental spectrum of  $\text{Hg}_2\text{X}_2$ , and the clear-cut spectroscopic manifestations of the phase transition (in particular, the narrowness of the soft-mode line, which makes it possible to trace the decrease of its frequency as  $T \rightarrow T_c^-$  to the lowest published value of several  $\text{cm}^{-1}$ ) make  $\text{Hg}_2\text{X}_2$  a convenient object for the study of general problems in structural phase transition in crystals.

The authors thank A. P. Levanyuk for a useful discussion and valuable remarks and M. E. Boiko and A. A. Vaipolin for reporting the results of the low-temperature x-ray structure investigations.

<sup>1</sup>Institute of Solid State Physics, Czechoslovak Academy of Sciences, Prague.

<sup>2</sup>Kazan' State University.

<sup>3</sup>We point out the (accidental?) proximity of two frequencies, of the deformation vibration  $\nu_2(E_g)$  and of the longitudinal vibration  $\nu_5^L(E_uLO)$ , which takes place for  $\text{Hg}_2\text{Cl}_2$  and  $\text{Hg}_2\text{Br}_2$ .

<sup>4</sup> $\epsilon_1 = \epsilon_{xx}$ ,  $\epsilon_2 = \epsilon_{yy}$ ,  $\epsilon_3 = \epsilon_{zz}$ ,  $\epsilon_4 = \epsilon_{yz}$ ,  $\epsilon_5 = \epsilon_{zx}$ ,  $\epsilon_6 = \epsilon_{xy}$ . The

stresses  $\sigma_i$  are similarly designated later on.

<sup>5</sup>Calculation shows that the ratio of the displacements of the Hg and Cl atoms for the transverse acoustic branch  $B_{3u}$  at the  $X_1$  point is 1.16, i.e., the  $\text{Hg}_2\text{Cl}_2$  molecules bend and assume a trapezoidal shape. As a result, the molecule chains that are linear at  $T > T_c$  acquire a "crankshaft" shape at  $T \leq T_c$  (Fig. 7).

<sup>6</sup>The measurements were performed by M. E. Boiko and A. A. Vaipolin at the A. F. Ioffe Physico-technical Institute.

<sup>1</sup>C. Barta, *Krist. Tech.* **5**, 541 (1970).

<sup>2</sup>H. Mark and J. Steinbach, *Z. Kristallogr.* **64**, 79 (1926).

<sup>3</sup>I. M. Sil'vestrova, Ch. Barta, G. F. Dobrzanskiĭ, L. M. Belyaev, and Yu. V. Pisarevskii, *Kristallografiya* **20**, 359 (1975) [*Sov. Phys. Crystallogr.* **20**, 221 (1975)].

<sup>4</sup>M. H. Dufett, *Bull. Soc. Franc. Mineralogie* **21**, 90 (1898).

<sup>5</sup>J. Petzelt, I. Mayerova, C. Barta, and L. Kislovskii, *Czech. J. Phys.* **B23**, 845 (1973).

<sup>6</sup>C. Barta, A. A. Kaplyanskiĭ, V. V. Kulakov, and Yu. F. Markov, *Opt. Spektrosk.* **37**, 95 (1974).

<sup>7</sup>C. Barta, A. A. Kaplyanskiĭ, V. V. Kulakov, and Yu. F. Markov, *Fiz. Tverd. Tela* **16**, 3125 (1974) [*Sov. Phys. Solid State* **16**, 2022 (1975)].

<sup>8</sup>C. Barta, A. A. Kaplyanskiĭ, V. V. Kulakov, and Yu. F. Markov, *Fiz. Tverd. Tela* **17**, 1129 (1975) [*Sov. Phys. Solid State* **17**, 717 (1975)].

<sup>9</sup>C. Barta, A. A. Kaplyanskiĭ, V. V. Kulakov, and Yu. F. Markov, *Pis'ma Zh. Eksp. Teor. Fiz.* **21**, 121 (1975) [*JETP Lett.* **21**, 54 (1975)].

<sup>10</sup>P. A. Fleury, J. F. Scott, and J. M. Worlock, *Phys. Rev. Lett.* **21**, 16 (1968).

<sup>11</sup>G. Ya. Lyubarskii, *Teoriya grupp i ee primeniya v fizike* (Group Theory and Its Applications in Physics), Fizmatgiz, 1957; O. V. Kovalev, *Neprivodimye predstavleniya prostranstvennykh grupp* (Irreducible Representations of Space Groups), AN USSR, 1961.

<sup>12</sup>A. P. Levanyuk and D. G. Sannikov, *Usp. Fiz. Nauk* **112**, 561 (1974) [*Sov. Phys. Usp.* **17**, 199 (1974)].

<sup>13</sup>H. Poulet and J.-P. Mathieu, *Lattice Dynamics of Vibration Spectra of Crystals*, Gordon, 1969.

<sup>14</sup>B. Z. Malkin, *Materialy 8 Vsesoyuznogo soveshchaniya po teorii poluprovodnikov* (Proc. 8-th All-Union Conf. on Semiconductor Theory), Kiev, 1975.

<sup>15</sup>E. F. Steigmeier and H. Auderset, *Solid State Commun.* **12**, 565 (1973).

Translated by J. G. Adashko